IOP Publishing Physica Scripta
Phys. Scr. 95 (2020) 065204 (17pp) https://doi.org/10.1088/1402-4896/ab793f

Stress-driven nonlocal elasticity for the instability analysis of fluid-conveying C-BN hybrid-nanotube in a magneto-thermal environment

Hamid M Sedighi[1,2,5], Hassen M Ouakad[3], Rossana Dimitri[4] and Francesco Tornabene[4]

[1] Mechanical Engineering Department, Faculty of Engineering, Shahid Chamran University of Ahvaz, Ahvaz, P.O. Box 61357-43337, Iran
[2] Drilling Center of Excellence and Research Center, Shahid Chamran University of Ahvaz, Ahvaz, 6135743337, Iran
[3] Mechanical and Industrial Engineering Department, College of Engineering, Sultan Qaboos University, P.O. BOX 33, Al-Khoud, Muscat, Oman
[4] Department of Innovation Engineering, University of Salento, 73100 Lecce, Italy

E-mail: h.msedighi@scu.ac.ir, houakad@squ.edu.om, rossana.dimitri@unisalento.it and francesco.tornabene@unisalento.it

Received 15 November 2019, revised 7 February 2020
Accepted for publication 24 February 2020
Published 6 April 2020

Abstract

The Eringen's strain-driven nonlocal differential model is well-established to exhibit inconsistencies when applied to bounded continua of applicative interest. The stress-driven nonlocal theory leads instead to well-posed nonlocal elastic formulations demonstrating stiffening structural responses. In the present article, using the stress-driven nonlocal model, a comprehensive analysis is conducted to explore the vibrational characteristics and critical divergence velocity of a hybrid-nanotube constructed by carbon (C) and boron nitride (BN) nanotubes conveying magnetic fluid. The impact of size-dependence, magnetic field and thermal medium on the dynamic behavior of the systems is included in the proposed model. The obtained governing equations of two-segment nanotubes are then examined using the finite element method. It is interestingly showed that the threshold of the divergence/flutter instability of the system would be enhanced by employing a hetero-nanotube instead of a nanotube composed of a uniform material. Furthermore, the results demonstrate that the configuration of the mode shapes may be dramatically changed for a nanotube conveying fluid. Therefore, the classical modes do no longer exist, and should not be considered in the dynamics of the system. It is also shown that by assuming a low temperature medium, the critical velocity increases by increasing the temperature and decreases in the case of high temperature.

Keywords: hybrid-nanotube, fluid-conveying, magnetic flow, stress-driven nonlocal model, magneto-thermal environment

(Some figures may appear in colour only in the online journal)

[5] Author to whom any correspondence should be addressed.

1. Introduction

Carbon nanotubes (CNTs) have outstanding mechanical, electronic and magnetic features that confer a great deal of employments in micro/nanoelectronic devices. Following the discovery of CNTs, several empirical investigations demonstrated the existence of another type of nanotubes constructed by boron and nitride atoms called boron-nitride nanotubes (BNNTs) with exceptional properties that introduce them as possible candidates to work in toxic, biological and high temperature media. Fortunately, the compatibility of the two structures, i.e. CNTs and their counterpart BNNTs, has motivated scientists to hybridize CNTs by BNNTs to create a new material platform with excellent properties which would simultaneously employ the benefits of carbon and boron nitride nanotubes [1, 2]. Thanks to the hollow cylindrical geometry of C-BN nanotubes, they are supposed to be potential candidates for nanopipes in nanofluidic systems with promising applications in targeted drug delivery or fluid filtration devices, biomimetic selective transport of ions among many. Rodríguez Juárez *et al* [3] examined the electronic/magnetic/mechanical features of different kind of hetero C-BN nanotubes and introduced the new composite nanotubes in drug delivery and nano-vehicle systems. Xiao *et al* [4] analyzed the conductance properties and transport features of the hybrid structures made of carbon and BN segments. Zhang and Wang [5] presented a beat-like behavior of carbon/BN nanotubes by adopting the continuum mechanics elasticity and verified their results with the molecular dynamics and showed that the interaction of two vibrational modes of the system results in fixing the intrinsic issues in the advancement of mass nanosensors. Vedaei *et al* [6] mathematically studied the sensing features of C-BN-C hybrid-nanotubes by performing the first principles density function theory together with the Green's function formalism theory. It was exhibited that O_2 and NO_2 molecules will chemically attract to the surface of hetero-nanotubes in which excellent selectivity can be predicted by collecting the signals of different electric fields. Chernozatonskii *et al* [7] considered the dimensionless and quasi one-dimensional hetero-nanotubes composed of C/BN fragments and computed their electron spectra by means of crystal orbitals. Cheng *et al* [8] studied the free vibration analysis of a hinged-hinged hetero-nanotube by assuming the equivalent Eringen nonlocal theory of elasticity and employed the dynamic stiffness method to analyze the mentioned structure. They concluded that the divergence instability of the system may be reduced by increasing the length ratio and the nonlocal parameters. Kiani [9] evaluated the frequencies of the stocky SWCNTs in a magnetic field for different boundary conditions considering nonlocal Timoshenko, Rayleigh and higher-order beam theories by utilizing a meshless method. He addressed the effect of small-scale parameter, strength of the magnetic field and the slenderness ratio of the SWCNT on the fundamental frequency of the actuated nanotube. In another research, Kiani [10] examined the influence of the longitudinal magnetic field on a system containing periodic jungles of single-walled carbon nanotubes to be able to explore the applicable ways of controlling the characteristics of transverse waves. He employed different nonlocal beam models and derived the discrete and continuous versions of equations of motion. Finally, he discussed the effects of system parameters like wavenumber, radius of SWCNTs, magnetic field strength, nonlocality on the flexural and shear frequencies and found that the longitudinal magnetic field could be employed as an efficient way to control characteristics of both flexural and shear waves in such conductive systems.

Over the past decade, several size-dependent continuum theories have been proposed by researchers to model the small scale behavior of nano-structures, including couple stress theories [11, 12], strain gradient theory [13, 14], Eringen's nonlocal elasticity [15–25] and energy-equivalent model (EEM) [26–29]. The most popular small-scale theory to capture the nanoscale behavior of miniature structures and systems is represented by the nonlocal elasticity theory. The strain-driven nonlocal theory is formulated using the Fredholm integral equation in which the nonlocal stress tensor at any point is considered as a weighted mean of the local strain tensor in the elastic body. In the case of unbounded domains, Eringen [25] proposed the mathematical kernel function to deal with the Rayleigh surface waves. In this kind of simplified nonlocal model, the nonlocal integral convolutions is replaced by the nonlocal differential equations. Therefore, the nonlocal differential elasticity theory can be employed as the equivalent and applicable mathematical framework taking into account the size-dependent behavior of nanoscale structures. Unfortunately, the equivalent model encountered some difficulties as applied to specific kind of boundary conditions and external loading and Eringen's nonlocal differential model shows somehow paradoxical results in dealing with bounded structural domains [30–32]. The stress-driven nonlocal model proposed by Romano and Barretta [33], instead, is characterized by alternating the roles of stress and strain tensors compared to the traditional Eringen nonlocal integral model. Consequently, the stress filed is defined by a Fredholm integral equation in which the strain field would be the result of an integral convolution of the local stress field and the nonlocal-dependent kernel function. Recently, the stress-driven nonlocal elasticity theory was efficiently implemented on different nanoscale systems and devices [34–40].

Owing to their approximately frictionless walls and excellent sensitivity in vibrational behavior, nanotubes conveying fluid can be utilized as biological channel, miniaturized drug delivery devices and fluid conveyors to achieve a higher critical velocity in such nanopipe-based systems [41–44]. Zhen and Fung [45] investigated the nonlinear vibrational response of fluid-conveying CNTs by means of Lindstedt–Poincaré asymptotic method. They took into account the harmonic excitation and geometric nonlinearity in the studied model in the context of nonlocal elasticity. Moreover, they considered the primary resonance of a simply supported system by examining the frequency-amplitude relationship and found that when the frequency of a forcing function tends to the fundamental frequency, the primary resonance of the first mode takes place, and as the ratio of the two lowest natural frequencies is close to 3,

the internal resonance phenomenon happens. Zhen and Fang [46] studied the effects of the nonlocal elasticity and thermal medium on the dynamic behavior of a CNT conveying fluid and analyzed the equations of motion with the aid of the differential quadrature method (DQM). They concluded that the effect of thermal gradient is to enhance the natural frequency and critical divergence velocity, and its impact decreases as the elastic medium surrounds the nanotube. By considering the nonlocal elasticity theory, Zhang *et al* [47] suggested the wave method to examine the vibrational characteristic of fluid-conveying CNTs. They presented the onset of divergence instability phenomenon and determined the critical velocity for different conditions of the system. Nematollahi *et al* [48] presented a mathematical model to investigate the small-scale dynamics of FG viscoelastic pipes considering the nonlocal strain gradient theory. They applied the Galerkin decomposition method to numerically solve the equations of motion and performed a comprehensive analysis to compute the divergence/flutter instability behavior of the considered system. Kiani [49] presented the dynamic interaction of stocky inclined SWCNT conveying fluid by using the Eringen's nonlocal elasticity. He employed the Timoshenko and higher-order beam theories to model the dynamics of the nanotubes and utilized the Galerkin method to discretize the governing equations. Finally, the effects of inclination angle, nonlocal parameter and slenderness ratio on the maximum amplitudes of longitudinal and transverse displacements were also discussed. Wang *et al* [50] investigated the capability of controlling the stability of fluid-conveying CNTs with the help of longitudinal magnetic field. They modeled the nanotube by adopting the nonlocal Euler–Bernoulli theory and discretized the equations of motion using the DQM. They demonstrated that the nonlocality of nanotube makes the system more flexible and can shift the unstable mode. Moreover, it was shown that the presence of a longitudinal magnetic field results in much stiffer CNT systems. Wang *et al* [51] studied the vibrational behavior of a SWCNT conveying fluid in a magneto-thermal environment. The effects of different parameters such as the fluid velocity and density, the temperature and magnetic field flux change, and the nonlocal parameter on the dynamic behavior of wavy CNTs were discussed. Hosseini *et al* [52] utilized the nonlocal beam theory to study the impact of a longitudinal magnetic field on the transverse vibration of a fluid-conveying SWCNT. They used the differential transformation method (DTM) to numerically solve the higher-order differential equations and discussed the effects of the nonlocal parameter and strength of the magnetic field on the divergence instability and natural frequency of SWCNTs. Their results exhibited that the critical flow velocity and fundamental frequency of SWCNTs will increase by increasing the nonlocal parameter.

As mentioned earlier and proved by many researchers, due to their outstanding properties, homogeneous nanotubes, i.e. BNNTs and CNTs, have potential applications in small-scale fluid-conveying systems. Therefore, it is convenient to fabricate a new hybrid structure composed of carbon/BN nanotubes for the next-generation nanopipe-based devices, wherein the features of both materials could be exploited simultaneously. Motivated by this inspiring idea, the present study deals with the instability and vibrational behavior of C-BN hybrid-nanotubes in a magneto-thermal environment by adopting the new size-dependent model. To this end, we formulate the stress-driven nonlocal theory of elasticity which is conveniently driven by the stress field and not by the elastic deformation and finite element method is used to analyze the governing equations of two fragments of nanotube. It is concluded that the nano-hetero-structure has higher critical velocity and natural frequency compared to the homogeneous nanotube. Finally, it is exhibited that the internal magnetic fluid may considerably change the mode shapes and therefore the classical mode shapes are no longer valid in dealing with such structures.

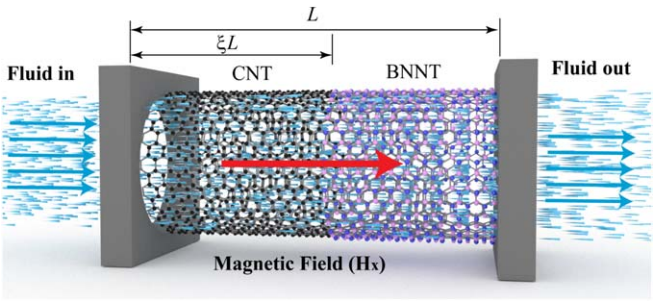

Figure 1. The schematic configuration of the hybrid nanotube conveying magnetic fluid.

2. Mathematical formulation

The considered hybrid-nanotube, as shown in figure 1, is composed of two different materials. The first part of the composite (hybrid) nanotube is a homogenous carbon nanotube and the second part is a boron nitride nanotube. It is assumed that the two segments have similar geometrical properties with different material constants. The nanotube has the total length L, $L_1 = \xi L, \quad 0 < \xi < 1$ and $L_2 = (1 - \xi)L$, represent the length of carbon and boron nitride nanotubes, respectively. The nanotube conveys a magnetic fluid flow and the boundary conditions of the nanopipe are clamped-clamped. The whole system is exposed to a horizontal magnetic field H_x and exposed to a thermal environment. It is worth noting that, since the longitudinal stiffness of nanotube is commonly much larger than its transverse stiffness, the transverse displacement of nanotube is remarkably higher than its longitudinal one [48]. On the other hand, the transverse motion of nanotube is usually supposed to be independent of its axial motion and therefore, in the current study, the transverse equation of motion is of interest.

2.1. Stress-driven nonlocal model

The nonlocal model introduced in this section is based on the stress-driven approach for describing the nonlocal elastic behavior. The first stress-driven formulation of the nonlocal model has been recently proposed as an alternative way compared to other strain-driven formulations [53]. In such

model the strain in a given point of the continuum $\boldsymbol{x}$ is a function of the entire stress field by the following convolution integral:

$$\varepsilon(x) = \int_V \varphi_\lambda(x, \bar{x})\, C(\bar{x}) \colon \sigma(\bar{x})\, d\bar{x} \tag{1}$$

where $\boldsymbol{C}$ is the elastic compliance $\boldsymbol{C} = E^{-1}$, and also in this case the kernel is an attenuation function of the space. Some advantages arise in this kind of formulation, one of those is the possibility to evaluate an analytical solution of the problem in a very simple way. In this section, we consider the bending problem formulation of a nonlocal Bernoulli-Euler nano-beam where the nonlocal behavior is modeled with the aid of a stress-driven formulation. In this case the only meaningful components of stress and strain are along the x-direction. Therefore, the nonlocal stress-strain relation is

$$\varepsilon(x) = \frac{1}{EI}\int_0^L \varphi_\lambda(x - \bar{x})\, \sigma(\bar{x})\, d\bar{x} \tag{2}$$

Moreover, as it has been shown previously [54, 55], for the bending problem at hand, equation (2) leads to the following bending curvature-moment relation:

$$\chi(x) = \frac{1}{EI}\int_0^L \varphi_\lambda(x - \bar{x})\, M(\bar{x})\, d\bar{x} \tag{3}$$

The advantage of this formulation is immediately shown if we consider the differential equation of the integral formulation. In particular, if the kernel is the attenuation function described by a bi-exponential function as:

$$\varphi_\lambda(x, \bar{x}) = \frac{1}{2L_c}\exp\left(-\frac{|x - \bar{x}|}{L_c}\right) \tag{4}$$

where nonlocal parameter is $\lambda = L_c/L$, being L_c a characteristic length, the differential formulation of the stress-driven nonlocal problem is given by:

$$\chi''(x) - \frac{1}{L_c^2}\chi(x) = -\frac{1}{EIL_c^2}M(x) \tag{5}$$

under the following boundary conditions:

$$BC\begin{cases} \chi'(0) = \dfrac{1}{L_c^2}\chi(0) \\ \chi'(L) = \dfrac{1}{L_c^2}\chi(L) \end{cases} \tag{6}$$

The above-mentioned stress-driven formulation is used to derive the governing equation for vibrating hybrid-nanotube conveying magnetic fluid flow.

2.2. Lorentz force

In this sub-section, we extract the differential form of Maxwell's equations and then acquire the Lorentz force relation arising from the longitudinal magnetic field. The Maxwell's relations for a conducting elastic body can be expressed as [56]:

$$\mathbf{J} = \nabla \times \mathbf{h} \tag{7}$$

$$\nabla \times \mathbf{E} = -\mu\frac{\partial \mathbf{h}}{\partial t} \tag{8}$$

$$\nabla.\mathbf{h} = 0 \tag{9}$$

$$\mathbf{E} = -\mu\left(\frac{\partial \mathbf{U}}{\partial t} \times \mathbf{H}\right) \tag{10}$$

$$\mathbf{h} = \nabla \times (\mathbf{U} \times \mathbf{H}) \tag{11}$$

in which $\mathbf{J}$, $\mathbf{h}$, $\mathbf{E}$ and $\mathbf{U}$ represent the current density, the disturbing vectors of magnetic field, the strength vectors of electric field and the displacement vector, respectively. Moreover, in the above equations, $\nabla = \frac{\partial}{\partial x}\hat{\mathbf{e}}_x + \frac{\partial}{\partial y}\hat{\mathbf{e}}_y + \frac{\partial}{\partial z}\hat{\mathbf{e}}_z$ is the Hamilton arithmetic operator and μ denotes the magnetic field permeability. Applying the longitudinal magnetic field $\mathbf{H} = (H_x, 0, 0)$ and considering the displacement vector as $\mathbf{U} = (0, v, w)$, the current density and the disturbing vectors of the magnetic field are written by:

$$\mathbf{h} = \nabla \times (\mathbf{U} \times \mathbf{H}) = -H_x\left(\frac{\partial v}{\partial y} + \frac{\partial w}{\partial z}\right)\hat{\mathbf{e}}_\mathbf{x} + H_x\frac{\partial v}{\partial x}\hat{\mathbf{e}}_\mathbf{y} + H_x\frac{\partial w}{\partial x}\hat{\mathbf{e}}_\mathbf{z} \tag{12}$$

$$\mathbf{J} = \nabla \times \mathbf{h} = -H_x\left(\frac{\partial^2 v}{\partial x \partial z} - \frac{\partial^2 w}{\partial x \partial y}\right)\hat{\mathbf{e}}_\mathbf{x} - H_x\left(\frac{\partial^2 v}{\partial y \partial z} + \frac{\partial^2 w}{\partial x^2} + \frac{\partial^2 w}{\partial z^2}\right)\hat{\mathbf{e}}_\mathbf{y} + H_x\left(\frac{\partial^2 v}{\partial x^2} + \frac{\partial^2 v}{\partial y^2} + \frac{\partial^2 w}{\partial y \partial z}\right)\hat{\mathbf{e}}_\mathbf{z} \tag{13}$$

Thereby, the Lorentz force denoted by $\mathbf{F}_L$ (a body force) induced by the longitudinal magnetic field can be obtained as:

$$\mathbf{F}_L = \mu(\mathbf{J} \times \mathbf{H}) = \mu H_x^2\left[\left(\frac{\partial^2 v}{\partial x^2} + \frac{\partial^2 v}{\partial y^2} + \frac{\partial^2 w}{\partial y \partial z}\right)\hat{\mathbf{e}}_\mathbf{y} + \left(\frac{\partial^2 w}{\partial x^2} + \frac{\partial^2 w}{\partial y^2} + \frac{\partial^2 v}{\partial y \partial z}\right)\hat{\mathbf{e}}_\mathbf{z}\right] \tag{14}$$

Since the current problem is assumed to be axisymmetric and the lateral displacement of C-BN nanotube is considered to be $w = w(x, t)$, the Lorentz force per unit length of the hybrid nanotube and in the z direction can be obtained as:

$$\mathbf{F}_L = F_{zL}\hat{\mathbf{e}}_\mathbf{z} = \mu A H_x^2\frac{\partial^2 w}{\partial x^2}\hat{\mathbf{e}}_\mathbf{z} \tag{15}$$

where A represents the nanotube cross section area.

2.3. Fluid-structure interaction in the presence of magnetic fluid

To derive the applied force due to the magnetic-fluid flow on the considered nanotube, it is assumed the internal viscous

fluid is laminar, incompressible and infinite passing through a nanotube with high aspect ratio. The momentum-balance relation governing the motion of the magnetic flow is expressed by the Navier–Stokes equation as:

$$\rho\frac{d\mathbf{v}}{dt} = -\nabla\mathbf{P} + \mu_s\nabla^2\mathbf{v} + \mathbf{J}\times\mathbf{H} \tag{16}$$

in which ρ and μ_s are the density and dynamic viscosity of fluid respectively, $\mathbf{P}$ denotes the fluid pressure, $\mathbf{v}$ is the velocity of fluid described by $\mathbf{v} = \bar{v}_x\hat{\mathbf{e}}_x + v_r\hat{\mathbf{e}}_r$. It is assumed that the radial component of the fluid velocity is equal to $v_r = dw/dt$ while the term $\bar{\mathbf{v}}_\mathbf{x}$ is the average flow velocity in the x-direction. The Lorentz force acting on the magnetic fluid due to the longitudinal magnetic field appeared in the last term of equation (16) is written by:

$$\mathbf{J}\times\mathbf{H} = \sigma(\mathbf{v}\times\mathbf{H})\times\mathbf{H} \tag{17}$$

where $\mathbf{J}$ and σ stand for the electric current density vector and the electrical conductivity of the fluid, respectively. In addition, the time derivative operator in equation (16) symbolized by d/dt is described by $d/dt = \partial/\partial t + \bar{v}_x\partial/\partial x$. Performing some mathematical computations and following the above-mentioned assumptions results in the governing equation for the pressure gradient of the magnetic fluid as:

$$\frac{\partial P}{\partial r} = -\rho\left(\frac{\partial^2 w}{\partial t^2} + 2\bar{v}_x\frac{\partial^2 w}{\partial x\partial t} + \bar{v}_x^2\frac{\partial^2 w}{\partial x^2}\right) + \mu_s\left(\frac{\partial^3 w}{\partial x^2\partial t} + \bar{v}_x\frac{\partial^3 w}{\partial x^3}\right) - \sigma H_x^2\left(\frac{\partial w}{\partial t} + \bar{v}_x\frac{\partial w}{\partial x}\right) \tag{18}$$

It was demonstrated by Wang and Ni [57] that the influence of fluid viscosity in the transverse load induced by a magnetic fluid on the nanotube can be neglected. Multiplying equation (18) by the cross section area of the internal fluid, A_f, yields the following relation for the force applied on the nanotube caused by the magnetic flow:

$$F_{mf} = -m_f\left(\frac{\partial^2 w}{\partial t^2} + 2\bar{v}_x\frac{\partial^2 w}{\partial x\partial t} + \bar{v}_x^2\frac{\partial^2 w}{\partial x^2}\right) - \sigma A_f H_x^2\left(\frac{\partial w}{\partial t} + \bar{v}_x\frac{\partial w}{\partial x}\right) \tag{19}$$

where m_f is the mass per unit length of the fluid. While we are dealing with the fluid flow at nanoscale, the average velocity of the fluid in nanotube is estimated through slip boundary conditions [52, 58]. According to the mentioned assumption, the average velocity correction factor (VCF), introduced by Rashidi *et al* [59], is employed to account for the effect of nanoscale on the fluid flow passing through a nanotube. They presented the following relation to calculate the VCF of the fluid:

$$VCF = \frac{\bar{v}_x}{\bar{v}_{x,(no-slip)}} = (1 + a_{Kn}Kn)\times\left(4\left(\frac{2-\sigma_v}{\sigma_v}\right)\left(\frac{Kn}{Kn+1}\right) + 1\right) \tag{20}$$

where $\bar{v}_x$ stands for the average flow velocity with the consideration of slip boundary conditions and $\bar{v}_{x,(no-slip)}$ denotes the averaged velocity of the fluid with no-slip boundary conditions. Furthermore, Kn represents the Knudsen number characterizing the boundary conditions and flow regimes, a_{Kn} is determined by Knudsen number and σ_v represents the tangential moment accommodation coefficient wherein is equal to 0.7 [59].

2.4. Applying stress-driven formulation in conjunction with the thermal effects

To extract the governing equation of motion, we consider a straight hybrid-nanotube under bending conditions with length L and cross-section A. The longitudinal axis of nanotube coincides with the x axis. According to the Bernoulli-Euler model, the relation between the curvature $\chi(x)$ and the flexural displacement w at any time is given by:

$$\chi(x) = \frac{\partial^2 w}{\partial x^2} \tag{21}$$

On the other hand, the d'Alembert dynamical equilibrium of a vibrating nanotube can be expressed by the following differential equation:

$$\frac{\partial^2 M}{\partial x^2} = -m\frac{\partial^2 w}{\partial t^2} + F_{ext} \tag{22}$$

where M denotes the resultant bending moment and m is the mass per unit length of the nanotube. In addition, F_{ext} is the total external force in z-direction due to the magnetic field effect and conveying fluid which can be written as follows:

$$F_{ext} = F_{zL} + F_{mf} \tag{23}$$

To derive the vibrational equation of motion, we take the second derivative of equation (5) with respect to x. One can obtain the following relation:

$$\frac{\partial^4\chi(x)}{\partial x^4} - \frac{1}{L_c^2}\frac{\partial^2\chi(x)}{\partial x^2} = -\frac{1}{EIL_c^2}\frac{\partial^2 M(x)}{\partial x^2} \tag{24}$$

and then using equation (21), the governing equation for the stress-driven vibrating nanotube conveying fluid can be obtained as follows:

$$EIL_c^2\frac{\partial^6 w}{\partial x^6} - EI\frac{\partial^4 w}{\partial x^4} = m\frac{\partial^2 w}{\partial t^2} - F_{ext} \tag{25}$$

Furthermore, based on the thermal elasticity theory, the axial force N_t due to the thermal effects can be expressed as [60]:

$$N_t = -\frac{EA}{1-2\upsilon}\alpha_x \Delta T \tag{26}$$

where υ is the Poisson's ratio of nanotube, α_x represents the coefficient of thermal expansion in x direction and ΔT denotes the temperature change. Taking into account the effect of thermal environment, the equation of motion governing the dynamic behavior of nanotube is re-formulated as:

$$EIL_c^2\frac{\partial^6 w}{\partial x^6} - EI\frac{\partial^4 w}{\partial x^4} = m\frac{\partial^2 w}{\partial t^2} - N_t\frac{\partial^2 w}{\partial x^2} - (F_{zL} + F_{mf}) \tag{27}$$

Moreover, the boundary conditions of the nanotube is doubly-clamped, and therefore the BCs of the structure are as follows:

$$w(0,\,t) = w(L,\,t) = \frac{\partial w(0,\,t)}{\partial x} = \frac{\partial w(L,\,t)}{\partial x} = 0 \tag{28}$$

2.5. Governing equations of motion

In the present sub-section, we aim to derive the governing equation of a hybrid C-BT nanotube conveying magnetic fluid by taking into consideration the nonlocal effects. As illustrated in equation (27) and using the related formulations for the external forces, the dynamic behavior of nanotube according to a classical EB beam model is governed by:

$$\begin{aligned} EIL_c^2\frac{\partial^6 w}{\partial x^6} - EI\frac{\partial^4 w}{\partial x^4} &= m\frac{\partial^2 w}{\partial t^2} + \frac{EA\alpha_x\Delta T}{1-2\upsilon}\frac{\partial^2 w}{\partial x^2} \\ &+ m_f\left(\frac{\partial^2 w}{\partial t^2} + 2(VCF)\bar{v}_{x,(no-slip)}\frac{\partial^2 w}{\partial x\partial t}\right. \\ &\left. + (VCF)^2\bar{v}^2_{x,(no-slip)}\frac{\partial^2 w}{\partial x^2}\right) + \sigma A_f H_x^2\left(\frac{\partial w}{\partial t}\right. \\ &\left. + (VCF)\bar{v}_{x,(no-slip)}\frac{\partial w}{\partial x}\right) - \mu A H_x^2\frac{\partial^2 w}{\partial x^2} \end{aligned} \tag{29}$$

It is assumed that the two parts of the nanotube have similar geometrical parameters and different material properties. Thus, by employing equation (29) for two sections of the nanotube and denoting the subscript 'BN' for boron-nitride and 'C' for carbon, one can obtain:

$$\begin{aligned} E_C IL_c^2\frac{\partial^6 w_1}{\partial x^6} &= E_C I\frac{\partial^4 w_1}{\partial x^4} + (m_C + m_f)\frac{\partial^2 w_1}{\partial t^2} \\ &+ \frac{E_C A\alpha_{xC}\Delta T}{1-2\upsilon}\frac{\partial^2 w_1}{\partial x^2} + m_f\left(2(VCF)\bar{v}_{x,(no-slip)}\frac{\partial^2 w_1}{\partial x\partial t}\right. \\ &\left. + (VCF)^2\bar{v}^2_{x,(no-slip)}\frac{\partial^2 w_1}{\partial x^2}\right) + \sigma A_f H_x^2\left(\frac{\partial w_1}{\partial t}\right. \\ &\left. + (VCF)\bar{v}_{x,(no-slip)}\frac{\partial w_1}{\partial x}\right) - \mu A H_x^2\frac{\partial^2 w_1}{\partial x^2} \quad \text{for} \quad 0 \leqslant x < \xi L \end{aligned} \tag{30}$$

$$\begin{aligned} E_{BN} IL_c^2\frac{\partial^6 w_2}{\partial x^6} &= E_{BN} I\frac{\partial^4 w_2}{\partial x^4} + (m_{BN} + m_f)\frac{\partial^2 w_2}{\partial t^2} \\ &+ \frac{E_{BN} A\alpha_{xBN}\Delta T}{1-2\upsilon}\frac{\partial^2 w_2}{\partial x^2} + m_f \\ &\left(2(VCF)\bar{v}_{x,(no-slip)}\frac{\partial^2 w_2}{\partial x\partial t} + (VCF)^2\bar{v}^2_{x,(no-slip)}\frac{\partial^2 w_2}{\partial x^2}\right) \\ &+ \sigma A_f H_x^2\left(\frac{\partial w_2}{\partial t} + (VCF)\bar{v}_{x,(no-slip)}\frac{\partial w_2}{\partial x}\right) \\ &- \mu A H_x^2\frac{\partial^2 w_2}{\partial x^2} \quad \text{for} \quad \xi L \leqslant x \leqslant L \end{aligned} \tag{31}$$

The following dimensionless parameters are introduced and the governing equations of motion can be expressed in non-dimensional form as follows:

$$\begin{aligned} &\bar{x} = \frac{x}{L},\ W_i = \frac{w_i}{L},\ \tau = t\sqrt{\frac{E_C I}{(m_C + m_f)L^4}},\ \beta = \frac{m_f}{m_f + m_C}, \\ &u = \bar{v}_{x,(no-slip)}L\sqrt{\frac{m_f}{E_C I}},\ \lambda_c = \frac{L_c}{L},\ \alpha_1 = \frac{E_{BN}}{E_C},\ \alpha_2 = \frac{m_{BN} + m_f}{m_C + m_f}, \\ &\bar{\alpha}_{xC} = \frac{\alpha_{xC}\Delta T}{1-2\upsilon}\frac{L^2}{r^2},\ \bar{\alpha}_{xBN} = \frac{\alpha_{xBN}\Delta T}{1-2\upsilon}\frac{L^2}{r^2}, \\ &h_{1x} = \frac{\sigma A_f H_x^2 L^2}{\sqrt{E_C I(m_C + m_f)}},\ h_{2x} = \frac{\sigma A_f H_x^2 L^2}{\sqrt{E_C I m_f}},\ h_{3x} = \frac{\mu A H_x^2 L^2}{E_C I}, \end{aligned} \tag{32}$$

in which r is the radius of gyration of the nanotube. By using the above-mentioned parameters, one can obtain:

$$\begin{aligned} \lambda_c^2\frac{\partial^6 W_1}{\partial\bar{x}^6} &= \frac{\partial^4 W_1}{\partial\bar{x}^4} + \frac{\partial^2 W_1}{\partial\tau^2} + \bar{\alpha}_{xC}\frac{\partial^2 W_1}{\partial\bar{x}^2} \\ &+ 2\sqrt{\beta}(VCF)u\frac{\partial^2 W_1}{\partial\bar{x}\partial\tau} + (VCF)^2 u^2\frac{\partial^2 W_1}{\partial\bar{x}^2} \\ &+ h_{1x}\frac{\partial W_1}{\partial\tau} + h_{2x}(VCF)u\frac{\partial W_1}{\partial\bar{x}} \\ &- h_{3x}\frac{\partial^2 W_1}{\partial\bar{x}^2}, \quad \text{for} \quad 0 \leqslant \bar{x} < \xi \end{aligned} \tag{33}$$

$$\alpha_1\lambda_c^2\frac{\partial^6 W_2}{\partial\bar{x}^6}=\alpha_1\frac{\partial^4 W_2}{\partial\bar{x}^4}+\alpha_2\frac{\partial^2 W_2}{\partial\tau^2}+\alpha_1\bar{\alpha}_{xBN}\frac{\partial^2 W_2}{\partial\bar{x}^2}.$$
$$+2\sqrt{\beta}(VCF)u\frac{\partial^2 W_2}{\partial\bar{x}\partial\tau}+(VCF)^2u^2\frac{\partial^2 W_2}{\partial\bar{x}^2}$$
$$+h_{1x}\frac{\partial W_2}{\partial\tau}+h_{2x}(VCF)u\frac{\partial W_2}{\partial\bar{x}}$$
$$-h_{3x}\frac{\partial^2 W_2}{\partial\bar{x}^2},\quad \text{for}\quad \xi\leqslant\bar{x}\leqslant 1 \tag{34}$$

Therefore, the following boundary/continuity conditions for C-BN hybrid nanotube are considered in the simulation processes:

$$W_1(0,\tau)=W_2(1,\tau)=\frac{\partial W_1(0,\tau)}{\partial\bar{x}}=\frac{\partial W_2(1,\tau)}{\partial\bar{x}}$$
$$=0,\quad \text{essential } \textit{boundary conditions} \tag{35}$$

$$\left.\begin{aligned}
&W_1(\bar{x},\tau)|_{\bar{x}=\xi}=W_2(\bar{x},\tau)|_{\bar{x}=\xi}\\
&\frac{\partial W_1(\bar{x},\tau)}{\partial\bar{x}}\bigg|_{\bar{x}=\xi}=\frac{\partial W_2(\bar{x},\tau)}{\partial\bar{x}}\bigg|_{\bar{x}=\xi}\\
&\lambda_c^2\frac{\partial^4 W_1(\bar{x},\tau)}{\partial\bar{x}^4}\bigg|_{\bar{x}=\xi}-\frac{\partial^2 W_1(\bar{x},\tau)}{\partial\bar{x}^2}\bigg|_{\bar{x}=\xi}=\alpha_1\lambda_c^2\frac{\partial^4 W_2(\bar{x},\tau)}{\partial\bar{x}^4}\bigg|_{\bar{x}=\xi}-\alpha_1\frac{\partial^2 W_2(\bar{x},\tau)}{\partial\bar{x}^2}\bigg|_{\bar{x}=\xi}\\
&\lambda_c^2\frac{\partial^5 W_1(\bar{x},\tau)}{\partial\bar{x}^5}\bigg|_{\bar{x}=\xi}-\frac{\partial^3 W_1(\bar{x},\tau)}{\partial\bar{x}^3}\bigg|_{\bar{x}=\xi}=\alpha_1\lambda_c^2\frac{\partial^5 W_2(\bar{x},\tau)}{\partial\bar{x}^5}\bigg|_{\bar{x}=\xi}-\alpha_1\frac{\partial^3 W_2(\bar{x},\tau)}{\partial\bar{x}^3}\bigg|_{\bar{x}=\xi}
\end{aligned}\right\}$$
continuity conditions at the junction of $\bar{x}=\xi$ (36)

In the next section, equations (33) and (34) are simultaneously solved by means of a Galerkin-based finite element method.

3. Solution methodology

The vibrational governing equation of C-BN hybrid nanotube conveying magnetic fluid in a thermal environment was given by equations (33) and (34) with the corresponding boundary/continuity conditions described in equations (35) and (36), Which can be decomposed via the finite element method. In this study, beam elements with two nodes and four degrees of freedom are employed. Thereby, the amplitudes of deflection and slope at each node are defined as follows:

$$d_1^e=W(\bar{x}_e=0),\quad d_2^e=\frac{\partial W}{\partial\bar{x}}\bigg|_{\bar{x}_e=0},$$
$$d_3^e=W(\bar{x}_e=l_e),\quad d_4^e=\frac{\partial W}{\partial\bar{x}}\bigg|_{\bar{x}_e=l_e} \tag{37}$$

in which l_e is the length of beam element. The following displacement function is adopted for the nanotube elements:

$$W_e(\bar{x})=a_1+a_2\bar{x}+a_3\bar{x}^2+a_4\bar{x}^3 \tag{38}$$

and the element nodal displacements at the two end nodes are defined by:

$$\{d_e\}^T=[d_1^e\ \ d_2^e\ \ d_3^e\ \ d_4^e] \tag{39}$$

Then the displacement function for each element can be expressed as:

$$W_e(\bar{x})=[N_1\ \ N_2\ \ N_3\ \ N_4]\{d_e\} \tag{40}$$

where

$$N_1=\frac{2\bar{x}_e{}^3-3\bar{x}_e{}^2l_e+l_e^3}{l_e^3},\quad N_2=\frac{\bar{x}_e{}^3l_e-2\bar{x}_e{}^2l_e^2+\bar{x}_el_e^3}{l_e^3}$$
$$N_3=\frac{-2\bar{x}_e{}^3+3\bar{x}_e{}^2l_e}{l_e^3},\quad N_4=\frac{\bar{x}_e{}^3l_e-\bar{x}_e{}^2l_e^2}{l_e^3} \tag{41}$$

The Galerkin weighted residuals method (GWRM) with the interpolation function N_i (as the weight function) can then be applied on equations (33) and (34). By assuming the solution of the problem in the following form:

$$W_i(\bar{x},\tau)=W_e^i(\bar{x})\exp(\lambda\tau),\ i=1,2 \tag{42}$$

and using the GWRM weak form of the equations of motion, one can obtain that:

$$[M]_e^C\ddot{W}_1+[D]_e^C\dot{W}_1+[K]_e^CW_1=0 \tag{43}$$

$$[M]_e^{BN}\ddot{W}_2+[D]_e^{BN}\dot{W}_2+[K]_e^{BN}W_2=0 \tag{44}$$

where

$$[M]_e^C=\int_0^{l_e}N^TN\,d\bar{x}$$
$$[D]_e^C=-2\sqrt{\beta}u(VCF)\int_0^{l_e}N^TN'd\bar{x}+h_{1x}\int_0^{l_e}N^TN\,d\bar{x}$$
$$[K]_e^C=-\lambda_c^2\int_0^{l_e}(N''')^TN'''\,d\bar{x}+\int_0^{l_e}(N'')^TN''\,d\bar{x}$$
$$-\bar{\alpha}_{xC}\int_0^{l_e}(N')^TN'\,d\bar{x}-u^2(VCF)^2\int_0^{l_e}(N')^TN'\,d\bar{x}$$
$$-h_{2x}u(VCF)\int_0^{l_e}N^TN'\,d\bar{x}+h_{3x}\int_0^{l_e}(N')^TN'\,d\bar{x} \tag{45}$$

$$[M]_e^{BN} = \alpha_2 \int_0^{l_e} N^T N \, d\bar{x}$$

$$[D]_e^{BN} = -2\sqrt{\beta}u(VCF)\int_0^{l_e} N^T N' \, d\bar{x} + h_{1x}\int_0^{l_e} N^T N \, d\bar{x}$$

$$[K]_e^{BN} = -\alpha_1\lambda_c^2\int_0^{l_e}(N''')^T N''' d\bar{x} + \alpha_1\int_0^{l_e}(N'')^T N'' \, d\bar{x} - \alpha_1\bar{\alpha}_{xBN}\int_0^{l_e}(N')^T N' \, d\bar{x} - u^2(VCF)^2\int_0^{l_e}(N')^T N' \, d\bar{x} - h_{2x}u(VCF)\int_0^{l_e} N^T N' \, d\bar{x} + h_{3x}\int_0^{l_e}(N')^T N' \, d\bar{x} - \tag{46}$$

In which the matrices [M], [D] and [K] represent the mass, damping and stiffness matrices, respectively. After applying the boundary/continuity conditions, by using the assumed solution and applying the usual assemblage procedure, the following equation is extracted:

$$(\lambda^2[M] + \lambda[D] + [K])\{\Delta_e\} = 0 \tag{47}$$

where λ and Δ_e are the eigenvalues and eigenvectors of the system. The eigenvalues of equation (47) might be complex numbers in general. Thus, to solve the eigen-problem (47), one can use the quadratic eigenvalue problem in the following form:

$$[A]\{\chi\} = \lambda[B]\{\chi\} \tag{48}$$

where

$$[A] = \begin{bmatrix} -[K] & [0] \\ [0] & [M] \end{bmatrix}, \quad [B] = \begin{bmatrix} [D] & [M] \\ [M] & [0] \end{bmatrix}, \quad \{\chi\} = \begin{Bmatrix} \Delta_e \\ \lambda\Delta_e \end{Bmatrix} \tag{49}$$

It should be pointed out that the solution of the characteristic equation (47) would be complex due to the presence of damping matrix [D]. Moreover, the real part of the eigenvector Δ_e is associated with the mode shape of the nanotube, whereas the real and imaginary parts of eigenvalues λ correspond to damping and natural frequencies of C/BN nanotube conveying fluid, respectively.

4. Results and discussion

In this section, in order to justify the soundness of the present work, some comparative studies are performed with the results of published works in the literature. Finally, the dynamic behavior of the system is presented by conducting some numerical examples and considering the natural frequencies, critical velocity and mode shapes of a C/BN hetero-nanotube.

4.1. Validation of the present analysis

To the best knowledge of the authors of this article, there is not any investigation on the dynamic analysis of doubly-clamped fluid-conveying C/BN hetero-nanotube in a magneto-thermal environment. Hence, in order to validate the results of the present study, we investigate the natural frequencies and divergence velocities of a homogeneous fluid-conveying CNT compared to the reported results from the literature. In addition, the properties of carbon and BN nanotubes are tabulated in table 1. A comparison between the first four natural frequencies and dimensionless divergence velocities of a clamped–clamped homogenous carbon nanotube are presented in table 2. The results are obtained by disregarding the nonlocal parameter and the magnetic/thermal environments. As indicated in this table, one can conclude that the natural frequencies and critical velocities of CNT agree very well with the values reported in [61–63]. Moreover, the variations of the divergence critical velocities of the first four modes of fluid-conveying carbon nanotube are presented in table 3. According to the results of table 3, one can see that the results of the current work are in good agreement with those reported in the literature.

Table 1. Properties of CNT and BNNT sections of hybrid nanotube.

Properties	CNT	BNNT
Density (rho) (g cm^{-3}) [8]	2.3	2.18
Young's modulus (E) (Tpa) [8]	1	1.8
Outer Radius (nm)	3.5	3.5
Thickness (h) (nm)	0.34	0.34
Aspect ratio ($L/2R_{out}$)	100	100
Coefficient of Thermal Expansion (Room Temperature) (K^{-1})	-1.6×10^{-6}	-0.3×10^{-6}
Coefficient of Thermal Expansion (High Temperature) (K^{-1})	1.1×10^{-6}	0.2×10^{-6}

4.2. The effect of length ratio

The impact of length ratio ξ on the natural frequencies, critical velocities and mode shapes of the fluid-conveying hybrid nanotubes are presented in this part. Figure 2 displays the real/imaginary parts of the non-dimensional frequencies of C/BN hybrid-nanotube versus the fluid velocity for three specific values of length ratio ξ. The parameter β is equal to 0.5, the length ratio is assumed to be 1, 0.8 and 0.5. From figure 2, it is found that the natural frequencies of the system increase with a decreased length ratio. This is due to the fact that the flexural rigidity of BN nanotube is higher than CNT. Furthermore, it is also concluded that the critical divergence velocity is increased by decreasing the length ratio ξ. This is a pleasant result for designing the composite nanopipes constructed from two-different materials that the divergence instability can be adjusted and fortunately the threshold of critical velocity can be postponed by reducing the length ratio ξ. Especially the following findings can be extracted from this figure. As the length ratio ξ is equal to 1, the first-mode divergence occurs when the non-dimensional velocity u approaches to 6.284; after that the 1st and 2nd flutter of the coupled-mode happens at $u = 9.265$. On the other hand, when the value of length ratio is equal to 0.8, the divergence of the 1st-mode occurs at $u = 6.761$ and when the fluid velocity raises to 9.759, the flutter of the coupled-mode takes place. Finally, when the length ratio

Table 2. Non-dimensional divergence critical velocity and the first four natural frequencies of a doubly-clamped CNT.

	Present study (100 nodes)	Reference [33]	Reference [34]	Reference [35]
Divergence critical velocity	6.284	6.284	6.29	6.3
1st natural frequency at zero flow velocity	22.37	22.3734	22.46	22.37
2nd natural frequency at zero flow velocity	61.67	61.6762	61.96	61.67
3rd natural frequency at zero flow velocity	120.93	120.9303	121.38	120.91
4th natural frequency at zero flow velocity	199.99	199.9905	—	—

Table 3. Variations of the divergence velocities of the four first modes for CNT versus parameter β.

Non-dimensional divergence velocity	Present study (100 nodes)		Reference [33]	
	$\beta = 0.1$	$\beta = 0.5$	$\beta = 0.1$	$\beta = 0.5$
Mode 1	6.284	6.284	6.284	6.284
Mode 2	8.988	—	8.989	—
Mode 3	12.570	12.570	12.572	12.572
Mode 4	15.461	—	15.466	—

takes the value $\xi = 0.5$, the divergence of the 1st mode takes place at $u = 7.069$ and by further increasing the flow velocity, the flutter of the coupled-mode happens at $u = 10.807$. Some further information can be inferred in figure 2 and left here for the sake of brevity. Additional findings about the divergence, re-stabilization and flutter phenomena for the other modes may be readily extracted by taking a glance into figure 2. The real/imaginary parts of the first five natural frequencies of the composite nanotube is illustrated in figure 3 for the same values of the length ratio when $\beta = 0.1$. The important result obtained from this figure is the fact that as the parameter β reduces, the divergence of the second mode occurs before the first-mode re-stabilization and the divergence velocity does not change. It is also demonstrated that the divergence of the 2nd mode is close to the coupled-mode flutter of the 1st and 2nd modes. Especially, one can see that for the case of $\xi = 1$, the 2nd mode divergence happens at $u = 8.988$, while by increasing the flow velocity to $u = 9.002$, the flutter of the coupled-mode occurs. As indicated in figures 3(b) and (c), one observes that when the parameter ξ takes the values 0.8and 0.5, the divergence velocities of the 2nd mode are increased and happen at $u = 9.390$ and $u = 10.460$, respectively.

The first five mode shapes of C/BN hybrid nanotube for three specific values of parameter ξ have been calculated using finite element method, as plotted in figure 4. It is noted that the slopes at different sections of the nanotube and the location of the maximum deflection changes and hence the configuration of the mode shape differs from that one of uniform CNT, where the maximum amplitude and node locations tend to move to the left support.

4.3. The effect of flow velocity

As a usual rule, many researchers frequently tend to utilize the classical mode shapes of nanotubes for examining the vibration characteristics nanotubes conveying fluid. However, the flow velocity inside the nanotube have a considerable impact on the configuration of the mode shapes and should be considered in the simulations. In order to examine the effects of the internal velocity on the mode shapes configuration, figure 5 depicts the variation of the first five modes for $\xi = 0.5$ and $\beta = 0.5$ and different values of u. It is evident that the increase of an internal fluid velocity u considerably changes the form of the mode shapes, thus leading to a significant change in values of the natural frequencies. It is interestingly concluded that the form of the mode shapes changes and occasionally reveals surprising results. For $u = 0$, as expected, the mode shapes are similar to those of classical hetero-nanotubes. It is particularly shown that as the flow velocity increases and takes the values $u = 4$, 7, the form of the first mode dramatically changes and evolves to a new configuration somehow similar to the second mode of classical hetero-nanotubes. According to the illustrated results of this figure, it is also found that the effect of the internal flow velocity is a considerable change in configurations of the mode shapes, especially for the first and second modes.

4.4. The effect of magnetic field

As mentioned earlier, BNNTs are isostructural to CNTs. It is evident that CNTs possess good magnetic properties, however, pristine BNNTs, in contrast to CNTs have relatively weak magnetic features. Nevertheless, several researchers proved that BNNTs can be functionalized into metallic/semi-metallic and even magnetic materials by partial hydrogenation, or embedding line defects or edge attachment of oxygen or sulfur atoms [64]. The influence of the length ratio ξ on the critical velocity of hybrid nanotube for three assigned values of non-dimensional parameter h_{2x} is depicted in figure 6. One can observe that the variation of critical velocity decreases non monotonically by increasing the length ratio. The effect of magnetic field is to increase the divergence critical velocity of the fluid-conveying C/BN nanotube.

4.5. The effect of temperature gradient

In order to explore the effect of the temperature gradient on the dynamic behavior of hetero-nanotube conveying fluid, in the current sub-section, the variation of the divergence critical

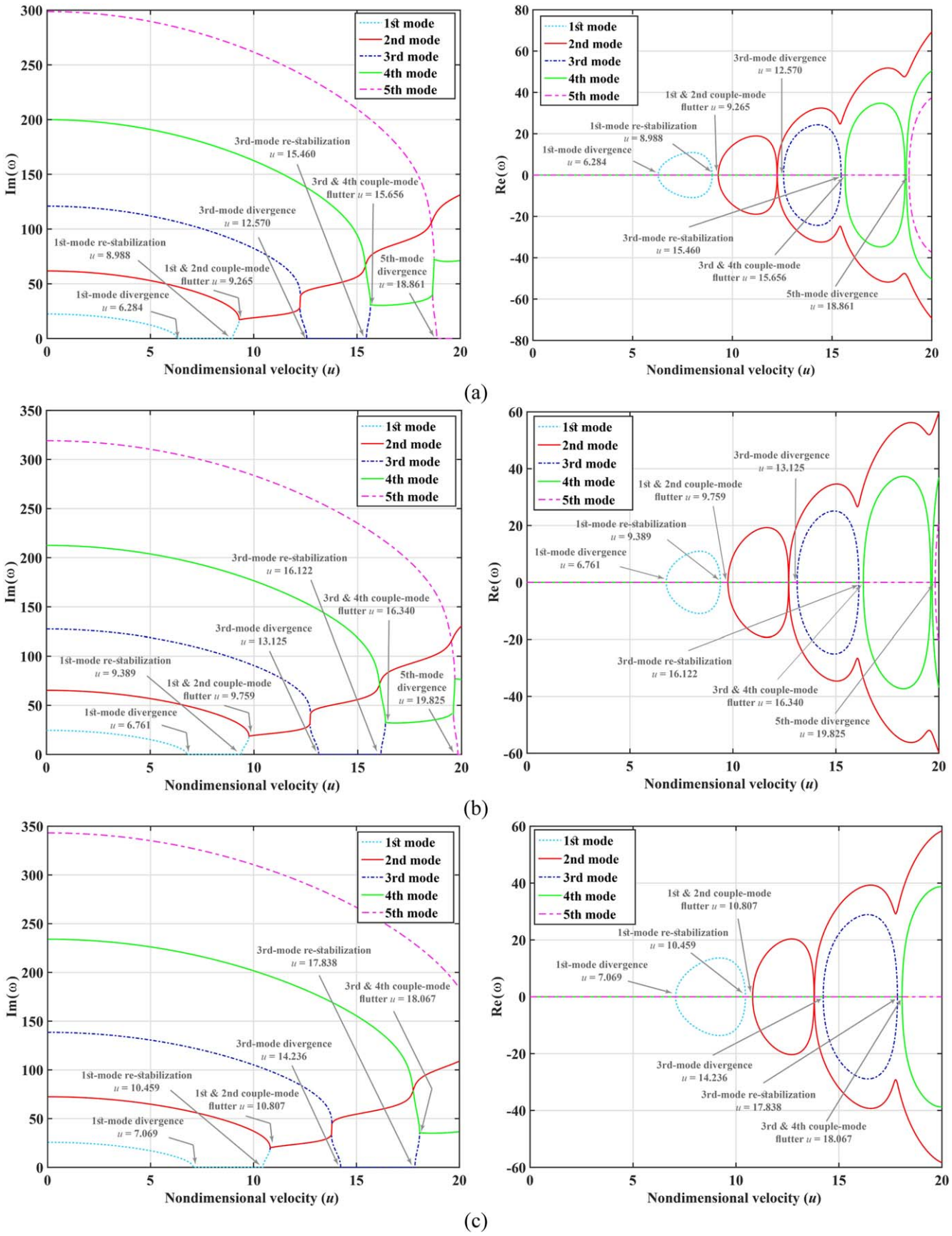

Figure 2. The variation of first five natural frequencies as a function of flow velocity (u) for $\beta = 0.5$. (a) $\xi = 1$ (b) $\xi = 0.8$ (c) $\xi = 0.5$.

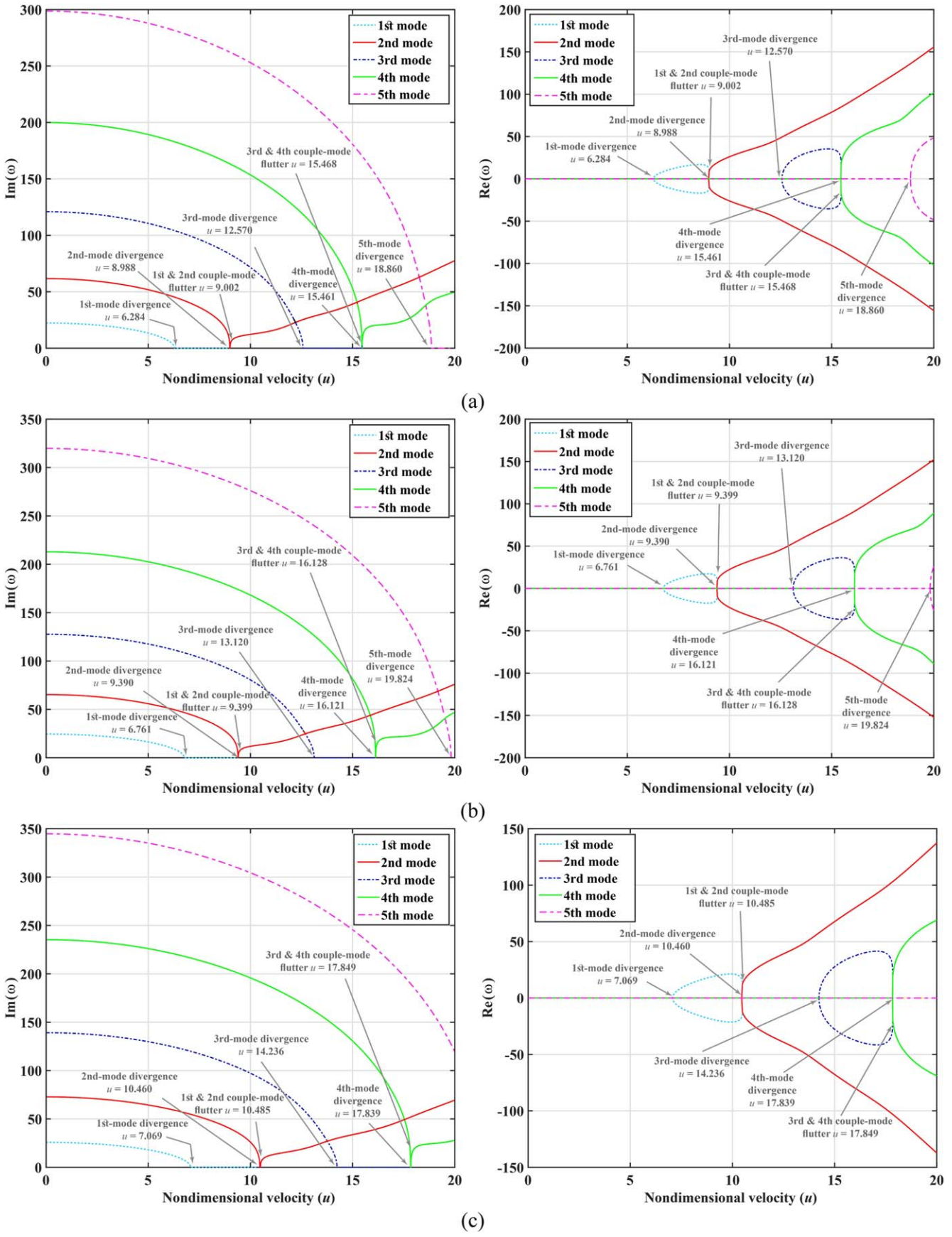

Figure 3. The variation of first five natural frequencies as a function of flow velocity (u) for $\beta = 0.1$. (a) $\xi = 1$ (b) $\xi = 0.8$ (c) $\xi = 0.5$.

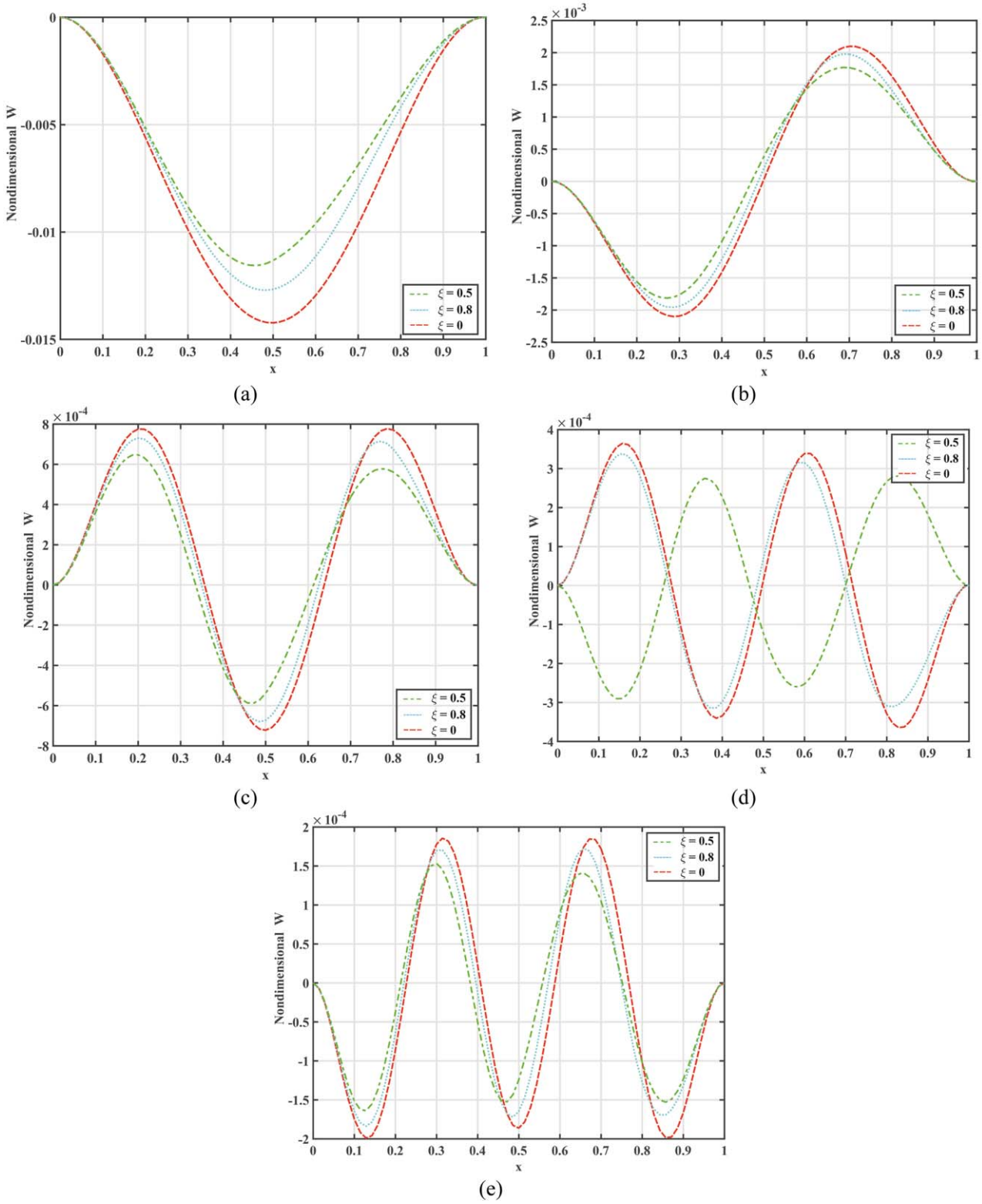

Figure 4. Comparison of the first five mode shapes of the hybrid nanotube at $u = 0$ for $\xi = 1$, $\xi = 0.8$ and $\xi = 0.5$ (a) first mode (b) second mode (c) third mode (d) fourth mode (e) fifth mode.

velocity versus the temperature changes is studied. Experimental findings exhibited that the coefficients of thermal expansion for both carbon and BN nanotubes take the negative values at low temperature conditions (<300 K) and shift to positive values at high temperature environment (>300 K) [18, 32]. To this end, the thermal expansion coefficients for carbon and boron-nitride segments at low and high temperature conditions are tabulated in table 1. For the case of room

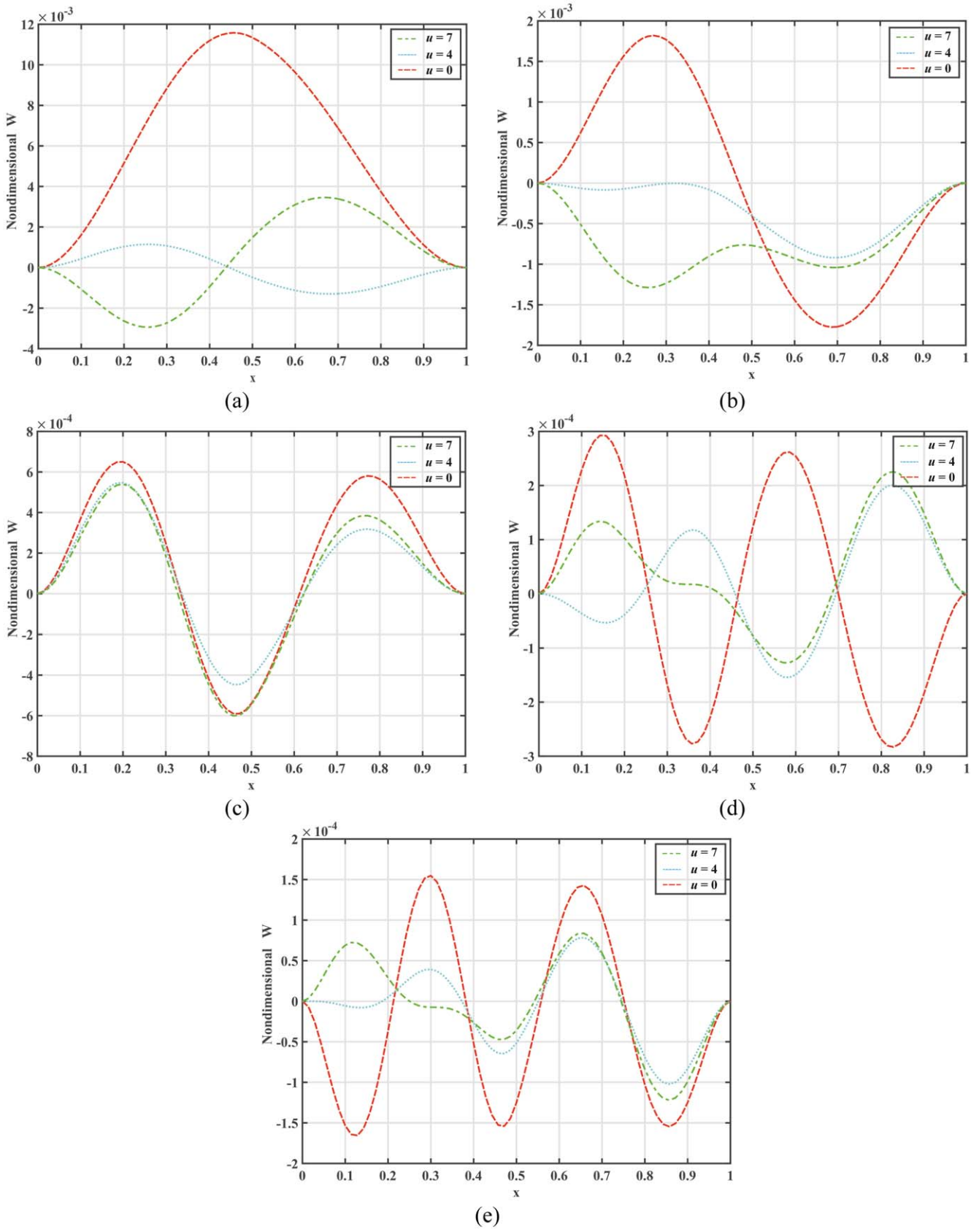

Figure 5. Comparison of the first five mode shapes of hybrid nanotube for $\xi = 0.5$ and $\beta = 0.5$ at different flow velocities (a) first mode (b) second mode (c) third mode (d) fourth mode (e) fifth mode.

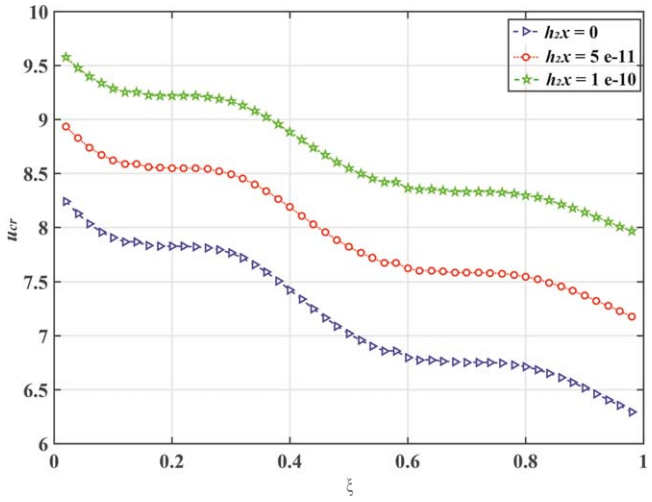

Figure 6. The variations of critical divergence velocity as a function of ξ for some assigned values of magnetic parameter h_{2x}.

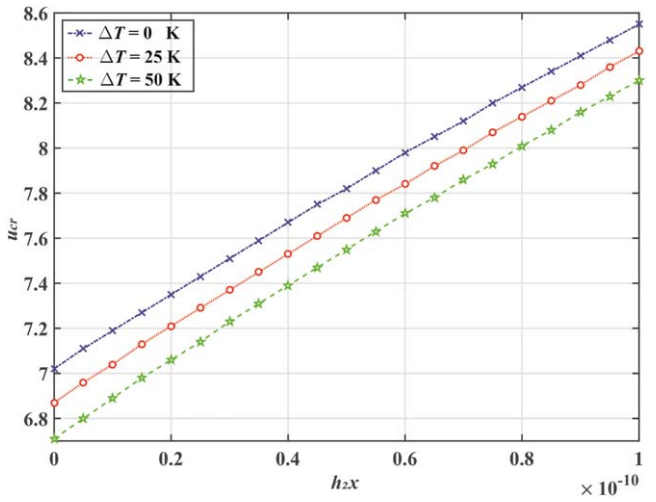

Figure 8. The variations of critical velocity as a function of h_{2x} for some assigned values of temperature change ΔT at high temperature conditions.

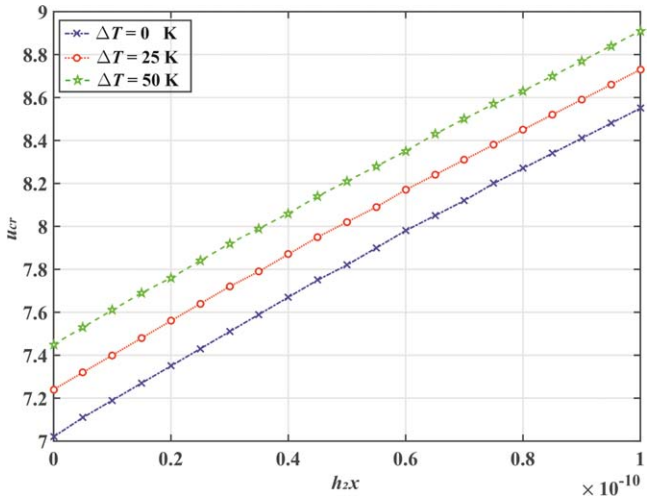

Figure 7. The variations of critical divergence velocity as a function of h_{2x} for some assigned values of temperature change ΔT at room temperature conditions.

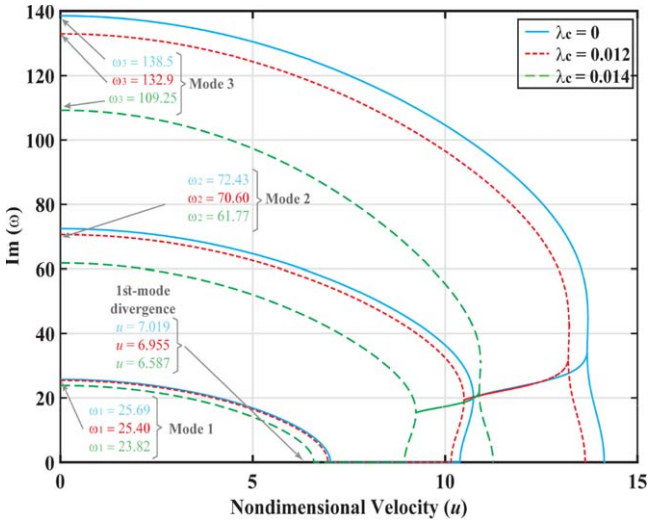

Figure 9. The variations of the lowest three natural frequencies for different values of nonlocal parameter λ_c.

(low) temperature, it is shown in figure 7 that higher temperature changes lead to a higher divergence velocity. The correlation between the critical velocity and the magnitude of magnetic field is almost linear. On the other hand, as demonstrated by the plotted curves in figure 8, for a high temperature environment, the effect of temperature gradient is to reduce the critical velocity which is totally in conflict with results of low temperatures.

4.6. The effect of stress-driven nonlocal theory

The effect of the nonlocal parameter λ_c on the variation of the three lowest natural frequencies of hetero-nanotubes is shown in figure 9. According the presented results, one can conclude that in presence of a nonlocal parameter, the values of the natural frequencies and the divergence velocities will be decreased and the effect of nonlocality is more pronounced for higher modes. Moreover, it is concluded that the sensitivity of this kind of nano-hetero-structure is increased for higher values of flow velocity. For instance, if the small-scale effect is ignored, the 1st mode divergence instability occurs at $u = 7.019$, while by taking into account the effect of size-dependency, i.e. at $\lambda_c = 0.014$, the first mode loses its stability when the internal flow velocity becomes $u = 6.587$.

5. Conclusions

The effect of the length ratio, magneto-thermal field and size-dependence on the divergence velocity, natural frequency and mode shapes of fluid-conveying C/BN hybrid-nanotube was examined in this work using a stress-driven-based nonlocal

model. The governing equations of two fragments of the composite nanotube were developed and numerically analyzed with the help of the finite element method. The obtained results are summarized as follows

1. The natural frequencies and the critical divergence velocities were enhanced by using hetero-nanotubes against the uniform one made of carbon atoms.
2. It was found that at low temperatures the divergence velocity is enhanced by any increase in the temperature. On the other hand, at high temperatures the temperature gradient reduces the critical velocity.
3. It was finally exhibited that by taking into account the effect of nonlocality, higher modes of hetero-nanotubes are more sensitive to the variation of the nonlocal parameter.

The results of this research study on employing the hybrid nanotubes would be of great interest in designing novel nanopipes and tuning the vibrational characteristics of biological devices composed of nanotubes.

Compliance with ethical standards

Conflict of interest

The authors declared no potential conflicts of interest with respect to the research, authorship and publication of this article.

Funding

The authors received no financial support for the research, authorship and publication of this article.

ORCID iDs

Hamid M Sedighi https://orcid.org/0000-0002-3852-5473
Hassen M Ouakad https://orcid.org/0000-0001-7262-2130

References

[1] Nozaki H and Itho S 1996 Lattice dynamics of a layered material BC2N *Physica B: Condensed Matter* **219–220** 487–9
[2] Stephan O, Ajayan P M, Colliex C, Redlich P, Lambert J M, Bernier P and Lefin P 1994 Doping graphitic and carbon nanotube structures with boron and nitrogen *Science* **266** 1683–5
[3] Juárez R, Chigo Anota A, Hernández Cocoletzi H, Sánchez Ramírez J F and Castro M 2017 Stability and electronic properties of armchair boron nitride/carbon nanotubes *Fullerenes, Nanotubes and Carbon Nanostructures* **25** 716–25
[4] Xiao H, Zhang C X, Zhang K W, Sun L Z and Zhong J X 2013 Tunable differential conductance of single wall C/BN nanotube heterostructure *Journal of Molecular Modeling* **19** 2965–9
[5] Zhang J and Wang C Y 2017 Beat vibration of hybrid boron nitride-carbon nanotubes—a new avenue to atomic-scale mass sensing *Computational Materials Science* **127** 270–6
[6] Vedaei S S and Nadimi E 2019 Gas sensing properties of CNT-BNNT-CNT nanostructures: a first principles study *Applied Surface Science* **470** 933–42
[7] Chernozatonskii L A, Gal'pern E G, Stankevich I V and Shimkus Y K 1999 Nanotube C–BN heterostructures: electronic properties *Carbon* **37** 117–21
[8] Cheng Q, Liu Y S, Wang G C, Liu H, Jin M G and Li M 2019 Free vibration of a fluid-conveying nanotube constructed by carbon nanotube and boron nitride nanotube *Physica E: Low-dimensional Systems and Nanostructures* **109** 183–90
[9] Kiani K 2015 Free vibrations of elastically embedded stocky single-walled carbon nanotubes acted upon by a longitudinally varying magnetic field *Meccanica* **50** 3041–67
[10] Kiani K 2019 Elastic waves in uniformly infinite-periodic jungles of single-walled carbon nanotubes under action of longitudinal magnetic fields *Journal of the Brazilian Society of Mechanical Sciences and Engineering* **41** 418
[11] Tadi Beni Y, Abadyan M and Koochi A 2011 Effect of the Casimir attraction on the torsion/bending coupled instability of electrostatic nano-actuators *Physica Scripta* **84** 065801
[12] Ghodrati B, Yaghootian A, Ghanbar Zadeh A and Mohammad-Sedighi H 2018 Lamb wave extraction of dispersion curves in micro/nano-plates using couple stress theories *Waves in Random and Complex Media* **28** 15–34
[13] Sedighi H M 2014 Size-dependent dynamic pull-in instability of vibrating electrically actuated microbeams based on the strain gradient elasticity theory *Acta Astronautica* **95** 111–23
[14] Tadi Beni Y and Abadyan M 2013 Size-dependent pull-in instability of torsional nano-actuator *Physica Scripta* **88** 055801
[15] Eltaher M A, Omar F A, Abdalla W S and Gad E H 2019 Bending and vibrational behaviors of piezoelectric nonlocal nanobeam including surface elasticity *Waves in Random and Complex Media* **29** 264–80
[16] Hamed M A, Sadoun M and Eltaher M A 2019 Effects of porosity models on static behavior of size dependent functionally graded beam *Structural Engineering and Mechanics* **71** 89–98
[17] Eltaher M A, Abdraboh A M and Almitani K H 2018 Resonance frequencies of size dependent perforated nonlocal nanobeam *Microsystem Technologies* **24** 3925–37
[18] Emam S A, Eltaher M A, Khater M E and Abdalla W S 2018 Postbuckling and free vibration of multilayer imperfect nanobeams under a pre-stress load *Applied Sciences* **8** 2238
[19] Kiani K 2018 Application of nonlocal higher-order beam theory to transverse wave analysis of magnetically affected forests of single-walled carbon nanotubes *International Journal of Mechanical Sciences* **138** 1–16
[20] Kiani K 2014 Free vibration of size-dependent magneto-electro-elastic nanobeams based on the nonlocal theory *Physica E: Low-dimensional Systems and Nanostructures* **63** 52–61
[21] Ansari R, Gholami R and Rouhi H 2015 Size-dependent nonlinear forced vibration analysis of magneto-electro-thermo-elastic Timoshenko nanobeams based upon the nonlocal elasticity theory *Composite Structures* **126** 216–26
[22] Kiani K 2018 Nonlocal free dynamic analysis of periodic arrays of single-walled carbon nanotubes in the presence of

longitudinal thermal and magnetic fields *Computers & Mathematics with Applications* **75** 3849–72
[23] Kiani K 2013 Vibration behavior of simply supported inclined single-walled carbon nanotubes conveying viscous fluids flow using nonlocal Rayleigh beam model *Applied Mathematical Modelling* **37** 1836–50
[24] Ghorbanpour Arani A, Haghparast E, Khoddami Maraghi K and Amir S 2015 Nonlocal vibration and instability analysis of embedded DWCNT conveying fluid under magnetic field with slip conditions consideration *Proceedings of the Institution of Mechanical Engineers, Part C: Journal of Mechanical Engineering Science* **229** 349–63
[25] Eringen A C 1972 Nonlocal polar elastic continua *International Journal of Engineering Science* **10** 1–16
[26] Mohamed N, Eltaher M A, Mohamed S A and Seddek L F 2019 Energy equivalent model in analysis of postbuckling of imperfect carbon nanotubes resting on nonlinear elastic foundation *Structural Engineering and Mechanics* **70** 737–50
[27] Eltaher M A *et al* 2019 Modal participation of fixed–fixed single-walled carbon nanotube with vacancies *International Journal of Advanced Structural Engineering* **11** 151–63
[28] Eltaher M A, Almalki T A, Almitani K and Ahmed K I 2019 Participation factor and vibration of carbon nanotube with vacancies *Journal of Nano Research* **57** 158–74
[29] Eltaher M A, Mohamed N, Mohamed S and Seddek L F 2019 Postbuckling of curved carbon nanotubes using energy equivalent model *Journal of Nano Research* **57** 136–57
[30] Barretta R, Faghidian S A and Luciano R 2019 Longitudinal vibrations of nano-rods by stress-driven integral elasticity *Mechanics of Advanced Materials and Structures* **26** 1307–15
[31] Barretta R, Caporale A, Faghidian S A, Luciano R, Marotti de Sciarra F and Medaglia C M 2019 A stress-driven local-nonlocal mixture model for Timoshenko nano-beams *Composites Part B: Engineering* **164** 590–8
[32] Barretta R, Faghidian S A and Marotti de Sciarra F 2019 Stress-driven nonlocal integral elasticity for axisymmetric nano-plates *International Journal of Engineering Science* **136** 38–52
[33] Romano G and Barretta R 2017 Stress-driven versus strain-driven nonlocal integral model for elastic nano-beams *Composites Part B: Engineering* **114** 184–8
[34] Barretta R, Fabbrocino F, Luciano R, de Sciarra F M and Ruta G 2019 Buckling loads of nano-beams in stress-driven nonlocal elasticity *Mechanics of Advanced Materials and Structures* ISSN: 1537-6494 (Print) 1537-6532 (https://doi.org/10.1080/15376494.2018.1501523)
[35] Barretta R, Faghidian S A, Luciano R, Medaglia C M and Penna R 2018 Free vibrations of FG elastic Timoshenko nano-beams by strain gradient and stress-driven nonlocal models *Composites Part B: Engineering* **154** 20–32
[36] Barretta R, Luciano R, Marotti de Sciarra F and Ruta G 2018 Stress-driven nonlocal integral model for Timoshenko elastic nano-beams *European Journal of Mechanics-A/Solids* **72** 275–86
[37] Barretta R, Fazelzadeh S A, Feo L, Ghavanloo E and Luciano R 2018 Nonlocal inflected nano-beams: a stress-driven approach of bi-Helmholtz type *Composite Structures* **200** 239–45
[38] Barretta R, Faghidian S A, Luciano R, Medaglia C M and Penna R 2018 Stress-driven two-phase integral elasticity for torsion of nano-beams *Composites Part B: Engineering* **145** 62–9
[39] Barretta R, Čanadija M, Feo L, Luciano R, Marotti de Sciarra F and Penna R 2018 Exact solutions of inflected functionally graded nano-beams in integral elasticity *Composites Part B: Engineering* **142** 273–86
[40] Barretta R, Čanađija M, Luciano R and Marotti de Sciarra F 2018 Stress-driven modeling of nonlocal thermoelastic behavior of nanobeams *International Journal of Engineering Science* **126** 53–67
[41] Majumder M, Chopra N, Andrews R and Hinds B J 2005 Nanoscale hydrodynamics: enhanced flow in carbon nanotubes *Nature* **44** 438
[42] Maraghi Z K, Arani A G, Kolahchi R, Amir S and Bagheri M R 2013 Nonlocal vibration and instability of embedded DWBNNT conveying viscose fluid *Composites Part B: Engineering* **45** 423–32
[43] Askari H and Esmailzadeh E 2017 Forced vibration of fluid conveying carbon nanotubes considering thermal effect and nonlinear foundations *Composites Part B: Engineering* **113** 31–43
[44] Chang T P 2013 Stochastic FEM on nonlinear vibration of fluid-loaded double-walled carbon nanotubes subjected to a moving load based on nonlocal elasticity theory *Composites Part B: Engineering* **54** 391–9
[45] Zhen Y X and Fang B 2015 Nonlinear vibration of fluid-conveying single-walled carbon nanotubes under harmonic excitation *International Journal of Non-Linear Mechanics* **76** 48–55
[46] Zhen Y X and Fang B 2010 Thermal–mechanical and nonlocal elastic vibration of single-walled carbon nanotubes conveying fluid *Computational Materials Science* **49** 276–82
[47] Zhang Z, Liu Y S and Lii B H 2014 Free vibration analysis of fluid-conveying carbon nanotube via wave method *Acta Mechanica Solida Sinica* **27** 626–34
[48] Nematollahi M S, Mohammadi H and Taghvaei S 2019 Fluttering and divergence instability of functionally graded viscoelastic nanotubes conveying fluid based on nonlocal strain gradient theory *Chaos* **29** 033108
[49] Kiani K 2014 Nanofluidic flow-induced longitudinal and transverse vibrations of inclined stocky single-walled carbon nanotubes *Computer Methods in Applied Mechanics and Engineering* **276** 691–723
[50] Wang L, Hong Y, Dai H and Ni Q 2016 Natural frequency and stability tuning of cantilevered CNTs conveying fluid in magnetic field *Acta Mechanica Solida Sinica* **29** 567–76
[51] Wang B, Deng Z, Ouyang H and Xu X 2015 Free vibration of wavy single-walled fluid-conveying carbon nanotubes in multi-physics fields *Applied Mathematical Modelling* **39** 6780–92
[52] Hosseini M and Sadeghi-Goughari M 2016 Vibration and instability analysis of nanotubes conveying fluid subjected to a longitudinal magnetic field *Applied Mathematical Modelling* **40** 2560–76
[53] Romano G and Barretta R 2017 Nonlocal elasticity in nanobeams: the stress-driven integral model *Int. J. Eng. Sci.* **115** 14–27
[54] Barretta R *et al* 2018 Exact solutions of inflected functionally graded nano-beams in integral elasticity *Compos Part B* **142** 273–86
[55] Barretta R *et al* 2018 Closed-form solutions in stress-driven two-phase integral elasticity for bending of functionally graded nano-beams *Physica E* **97** 13–30
[56] Narendar S, Gupta S S and Gopalakrishnan S 2012 Wave propagation in single-walled carbon nanotube under longitudinal magnetic field using nonlocal Euler–Bernoulli beam theory *Applied Mathematical Modelling* **36** 4529–38
[57] Wang L and Ni Q 2009 A reappraisal of the computational modelling of carbon nanotubes conveying viscous fluid *Mechanics Research Communications* **36** 833–7
[58] Sadeghi-Goughari M, Jeon S and Kwon H J 2017 Effects of magnetic-fluid flow on structural instability of a carbon

nanotube conveying nanoflow under a longitudinal magnetic field *Physics Letters A* **381** 2898–905
[59] Rashidi V, Mirdamadi H R and Shirani E 2012 A novel model for vibrations of nanotubes conveying nanoflow *Computational Materials Science* **51** 347–52
[60] Wang L, Ni Q, Li M and Qia Q 2008 The thermal effect on vibration and instability of carbon nanotubes conveying fluid *Physica E* **40** 3179–82
[61] Zare A, Eghtesad M and Daneshmand F 2017 Numerical investigation and dynamic behavior of pipes conveying fluid based on isogeometric analysis *Ocean Engineering* **140** 388–400
[62] Lee H L and Chang W J 2008 Free transverse vibration of the fluid-conveying single-walled carbon nanotube using nonlocal elastic theory *Journal of Applied Physics* **103** 024302
[63] Rafiei M, Mohebpour S R and Daneshmand F 2012 Small-scale effect on the vibration of non-uniform carbon nanotubes conveying fluid and embedded in viscoelastic medium *Physica E* **44** 1372–9
[64] Zhang Z, Liu X, Yu J, Hang Y, Li Y, Guo Y, Xu Y, Sun X, Zhou J and Guo W 2016 Tunable electronic and magnetic properties of two-dimensional materials and their one-dimensional derivatives *WIREs Computational Molecular Science* **6** 324–50